Aus dem Zentrum für Neurologie Tübingen

Neurologische Klinik und Hertie-Institut für klinische Hirnforschung

Abteilung Kognitive Neurologie

Ärztlicher Direktor: Professor Dr. H.-P. Thier

How precise is gaze following in humans?

Inaugural-Dissertation
zur Erlangung des Doktorgrades
der Medizin

der Medizinischen Fakultät
der Eberhard-Karls-Universität
zu Tübingen

vorgelegt von

Simon Walter Bock

aus

Tübingen

2009

Dekan:	Professor Dr. I. B. Autenrieth
1. Berichterstatter:	Professor Dr. H.-P. Thier
2. Berichterstatter:	Professor Dr. U. Schiefer

Meinen Eltern

Diese Arbeit wurde im Fachjournal „Vision Research“ veröffentlicht:

Bock SW, Dicke P, Thier P.
How precise is gaze following in humans?
Vision Res. 2008 Mar; 48 (7): 946 - 957.

Herrn Prof. Thier danke ich für die Überlassung des Arbeitsplatzes und des Themas der vorliegenden Arbeit sowie für zahlreiche, wertvolle Anregungen und Diskussionen.

Besonders herzlich möchte ich mich bei der Arbeitsgruppe für das gute Arbeitsklima und für die vielen anregenden Diskussionen bedanken.

Meiner Frau danke ich für viele wertvolle Anregungen und ihre große Geduld.

Mein besonderer Dank gilt den ‚Sendern’ und ‚Empfängern’, ohne deren aufmerksamen Blick diese Arbeit nicht möglich gewesen wäre.

Wie präzise ist „gaze following“ beim Menschen ?

Abstract der Dissertation von S. W. Bock

„Gaze following” (das Erkennen des Blickziels seines Gegenübers an dessen Blick) ist die Basis von gemeinsamer visueller Aufmerksamkeit („joint visual attention“). Gemeinsame Aufmerksamkeit kann als Grundlage der Erkenntnis eines anderen Individuums als sich seiner selbst bewußt angesehen werden. Bisher ist die Kenntnis um die Präzision von „gaze following“ sehr beschränkt. Wir haben die Fähigkeit menschlicher ‚Empfänger’ untersucht, ein Objekt aus einer Anzahl gleichartiger Objekte auszuwählen, das durch den Blick eines menschlichen oder durch den Computer dargestellten ‚Senders’ definiert wurde. Sender und Empfänger saßen einander in 1 Meter Abstand gegenüber und schauten sich durch einen Ring von 90 Stecknadelkopf-Objekten in ihrer Mitte an. Der Empfänger identifizierte das vom Sender gewählte Objekt anhand dessen Blickrichtung. Mit dieser Versuchsanordnung war es erstmals möglich, nicht nur horizontale und vertikale, sondern Abweichungen des Empfängerblicks in alle Raumrichtungen zu bestimmen.

Die Abweichungen des Empfängers vom Blickziel des Senders waren normalverteilt und die Treffgenauigkeit war sehr hoch. Die Präzision von „gaze following“ unterschied sich nicht für monokular oder binokular sehende Empfänger, jedoch war die Erkennungsleistung schlechter wenn nur ein Auge des Senders sichtbar war. Zwei Arten systematischer Abweichung konnten identifiziert werden: ein „upward bias“ (eine Tendenz der Blickrichtung nach oben) und ein „cardinal-axis bias“ (eine Tendenz der Blickrichtung zu den Hauptachsen).

Anhand der identifizierten Abweichungen kann in weiteren Versuchen das Referenzsystem (Sender-, Welt- oder Empfängerkoordinaten) bestimmt werden, das beim Verfolgen des Blicks eines Gegenübers benutzt wird, was letztlich die Suche nach einem neuralen Korrelat von “gaze following” erleichtern könnte. Zusammenfassend ist „gaze following“ beim Menschen nicht nur sehr genau, sondern auch überraschend robust gegenüber Manipulationen der Sender-Signale, welche die Augen des Empfängers leiten.

How precise is gaze following in humans ?

Simon W. Bock*, Peter Dicke and Peter Thier

Department of Cognitive Neurology, Hertie-Institute for Clinical Brain Research,

University of Tübingen, Hoppe-Seyler-Str. 3, 72076 Tübingen, Germany

Key words:

attention, gaze following, triadic eye gaze, social interaction, eye movements

* Corresponding author:

Simon W. Bock

Email address: sbock@uni-tuebingen.de

Telephone: +49-7071-2980469

Mobile: +49-179-6613883

Fax: +49-7071-294617

Contents

Abstract 4
1. Introduction 5
2. Methods 8
2.1. Setup 8
2.2. Participants 9
2.3. Design 9
2.3.1. Human sender 11
2.3.2. Computer-presented image of sender 11
2.4. Definitions 12
2.5. Data analysis 13
2.5.1. Comparison of conditions: global precision 13
2.5.2. Target position dependent (local) analysis 13
2.5.3. Modelling of bias components 14
3. Results 16
3.1. Comparison of conditions: global precision 16
3.2. Local precision anisotropy 19
3.3. Upward bias 20
3.4. Cardinal-axis bias 21
3.5. Estimates obtained by modelling local bias and local precision 23
4. Discussion 25
4.1. Comparison of global precision to previous studies 25
4.2. Local precision anisotropy is in line with previous studies 28
4.3. Receivers' bias in upward direction 29
4.4. Receivers' bias towards the cardinal axes 30
4.5. In which frame of reference is gaze following coded? 31
5. Conclusion 34
Acknowledgements 35
References 36

Abstract

Gaze following is the basis of joint visual attention. We investigated the capability of human ‘receivers’ to single out one of many objects, defined by the gaze of a human or computer ‘sender’. Deviations from the sender’s target were normally distributed and judgements were highly accurate. Accuracy of gaze following under binocular and monocular vision of the receiver did not differ, but performance was poorer when only one of the sender’s eyes was visible. Two types of systematic bias could be identified: upward bias and cardinal-axis bias. In summary, human gaze following is not only very precise but also surprisingly robust to manipulations of the sender cues available for guiding the receiver’s eyes.

1. Introduction

The direction of a person's gaze indicates what object he or she is paying attention to and a shift in gaze direction indicates a change of the object of attention. Therefore, gaze direction may serve as a key to developing an understanding of the other person's interests and possible intentions. Indeed, humans make use of eye-gaze, i.e. the orientation of someone else's eyes relative to objects in the world, very early during development. Newborns already distinguish another person's face, and from birth on babies look longer at facial photographs depicting direct gaze than at ones depicting averted gaze (Farroni, Csibra, Simion, & Johnson, 2002): they start to engage in a *dyadic* interaction, *mutual gaze* between baby and mother. Hints on the influence of *dyadic* interaction on neural processing range from a suppression of cortically evoked brain stem potentials in the macaque when the animal detects being watched (Wada, 1961) to an altered correlation between attractiveness rating and fMRI signal in humans through the perceived eye contact of facial photographs with the subject (Kampe, Frith, Dolan, & Frith, 2001). Later in life, infants interact with objects and people in a *triadic* way. This can result in a referential triangle between child, mother and an object of mutual interest (also termed *joint attention*). Although attention does not depend on visual fixation, the simplest form is *joint visual attention*, or "looking where someone else is looking" i.e., *gaze following* (Butterworth, 1991, p. 223). According to Baron-Cohen, joint attention is the key prerequisite for the development of a *'theory of mind'* (Baron-Cohen, 1994); an ability normal children have mastered by the age of 4 years. Children with autism show deficits in this ability, which might be partially due to their inattention to faces and eye-gaze (Dalton et al., 2005). Hence, the main function of dyadic gaze is to regulate face-to-face social interaction, whereas triadic gaze involves a third party as the focus of attention of the sender (Symons, Lee, Cedrone, & Nishimura, 2004).

Gaze following has been investigated in a qualitative manner in both human and non-human primates (Emery, 2000). However, a quantitative measure of

gaze following judgements is indispensable for the understanding of the underlying neural circuitry. Three studies examined *dyadic* gaze, and gaze towards virtual targets, in a quantitative manner: Gibson & Pick (1963) reported the precision (standard deviation) of a human receiver in distinguishing whether he was being looked at by a human sender (whose gaze was directed either at the receiver's nasion or horizontally displaced from it). Cline (1967) examined horizontal and vertical displacement of a sender's gaze from the receiver's nasion. To some extent he examined *triadic* gaze, because his sender looked at objects (a 'third party', although invisible to the receiver), and his receivers not only assessed being looked at but also indicated perceived gaze direction by pointing towards a transparent response board. But still, sender and receiver could not share *joint visual attention.* Finally, Anstis, Mayhew, & Morley (1969) compared the relationship of the actual to the perceived direction of gaze and modelled the function relating sender positions to receiver responses for the first time. Their work was based on gaze towards virtual targets as well, and limited to eccentricities along a linear scale. *Triadic* gaze in the sense that joint objects are attended to by both the sender and the receiver was only studied recently by Symons et al. (2004), who also limited themselves to targets arranged on a horizontal bar (now below the line of eye contact). Because they used a two alternative forced choice task (whether the sender was looking left or right of a given target), a standard psychophysical function could be applied for analysis. However, this also necessitated different target distances for different conditions and prevented the analysis of local bias components. While previous studies used horizontal and vertical scales for their analysis, in which the gaze angles are wider at the ends in a nonlinear fashion, the present setup has the convenient feature that all targets correspond to equally spaced visual gaze angles between neighbouring targets. The findings of these studies will be related to our results in more detail in the discussion.

The present study assessed the ability of a *receiver* to judge which *object,* singled out of an array of identical objects, a *sender* was gazing at. Receivers' performances were tested under different conditions, A) the receiver following

the sender's saccade to assess the benefit of dynamic stimuli, B) the object defined by static gaze to achieve more controlled conditions, C) monocular vision on the receiver's side to test if binocular disparity cues are used, D) monocular visibility on the sender's side to evaluate if information gained from both eyes is utilised and E) computer-presented photographic images replacing the sender to have identical stimulation across subjects. This experimental system allowed us, for the first time, to study gaze following towards objects positioned at all spatial angles in respect to the sender's eyes, due to a circular arrangement of response targets, measuring precision for horizontal, vertical as well as diagonal offsets. We found that performance varied depending on the target position. Furthermore, two types of systematic bias were observed to be associated with the anisotropy in precision: *upward bias* and *cardinal-axis bias*. These might be used in further work to establish the frame of reference of gaze following, which will help identify the sensorimotor networks involved.

2. Methods

2.1. Setup

To measure triadic gaze perception accuracy in near space, the setup outlined in Fig. 1 was developed. A person acting as *sender* cued the location of one out of 90 target objects by looking at it with an isolated eye movement. A second person, the *receiver*, tried to follow the sender's gaze and reported the target at which he judged the sender to be gazing. Target *objects* were pinheads numbered from one to ninety, arranged on a ring placed midway between the participants at 50 cm distance to each of them (object size 0.44° visual angle, object spacing 1.03°, ring radius 15°). Based on preliminary tests, object spacing had been chosen in a way that roughly 85% of receivers' reports of the target differed from the object gazed at by the sender. The line of eye-contact between sender and receiver was adjusted to traverse the centre of the ring with the help of head and chin rests, fixing both heads to a frontal orientation.

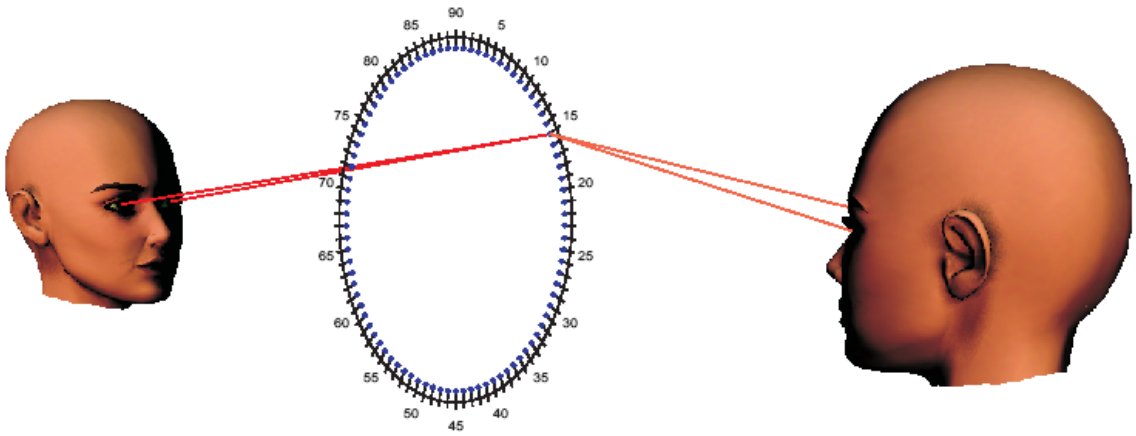

Fig. 1. Sender and receiver facing each other at 100 cm distance with a ring of 90 pinhead objects placed midway between them (object size 0.44° visual angle, object spacing 1.03°, ring diameter 30°). Their line of eye-contact was adjusted to the centre of the ring with the help of head and

chin rests, fixing both heads to a frontal orientation. Lines indicate sender's and receiver's gaze to pinhead number 15.

2.2. Participants

Twelve adults (age 27.2 ± 6.6 years; six males) participated in the experiment as receivers, interacting with two adult senders (age 28 and 30 years). Nine of the receivers were naive to the purpose of the experiment. The senders were a blue-eyed female and a brown-eyed male with no ocular imbalance as assessed ophthalmologically. All participants had normal or corrected-to-normal vision.

Receivers stated to have followed different strategies of gaze behaviour, most prominently a) looking at the sender's face up to his saccade, then following his gaze to the target object and indicating its number, or b) looking repeatedly back and forth between the sender's eyes and the probable target. We did not formally investigate receiver's gaze behaviour; on provisional account there did not seem to be a profound difference in performance between these strategies.

2.3. Design

For each trial, a target object was conveyed to the sender by specifying its number via headphones. The sender then directed his gaze to it and maintained fixation until the receiver answered (Fig. 2). The target list was randomly permuted to ensure that all target positions were covered. The receiver indicated the number of the perceived target on a computer keyboard. Performance was tested under five different conditions, run in randomized order for each receiver:

A) 'dynamic' – The receiver followed the sender's saccade from the receiver's nasion to the target. He was allowed to use binocular vision, and both sender's eyes were visible.

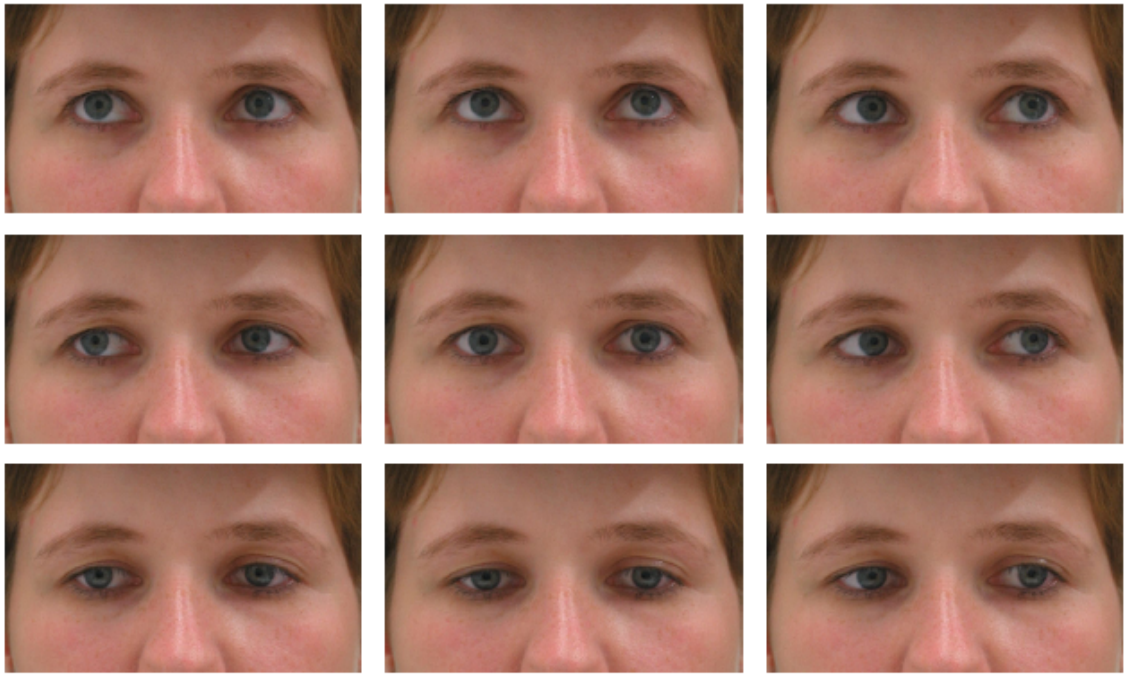

Fig. 2. Sender's eyes, arranged according to gaze directed at selected targets on the setup ring. Central photograph: direct gaze at receiver's nasion; top left: gaze at central target of top left quadrant, as defined in 2.5.2; top: gaze at topmost target; top right: gaze at central target of top right quadrant; etc. The images comprise the eye region of actual 'computer sender' photographs.

B) 'static' – The receiver was limited to follow the gaze cue of the sender's eyes only after the sender had achieved stable fixation of the target as indicated by an acoustic GO-signal.

C) 'receiver monocular' – The receiver was limited to monocular vision by an occluder, obscuring the view of the left eye in one and of the right eye in another session. Otherwise, the same sequence as in 'static' was used.

D) 'sender monocular' – The receiver was limited to see only one eye of the sender by an occluder in front of the sender's left eye in one and right eye in another session. Otherwise, the same sequence as in 'static' was used.

E) 'computer sender' – Computer-presented photographic images were used as sender, in place of the human.

The two *monocular* conditions (C and D) comprised two sessions of 90 trials each, for the left and for the right eye, respectively. The other three conditions (A, B and E) consisted of 90 trials, each.

2.3.1. Human sender

For the first four conditions, two human subjects (sender and receiver) sat with their heads on chin-rests, facing each other at a distance of 100 cm, the ring of target objects placed midway between them. Their chin-rests were adjusted to assure the same height for both participants' eyes and the centre of the ring. One of the senders had normal vision, the other was corrected to normal by contact lenses.

2.3.2. Computer-presented image of sender

In the last condition, the sender was replaced by digitized photographic images of a sender's face, one for each gaze direction. The images were presented on a computer screen at 1:1 magnification (14 × 19 cm ≡ 530 × 730 pixels). The pupils had 0.4 cm diameter, the irises 1.2 cm diameter, and were arranged in eye regions measuring 2.8×1.2 cm (the height of the eye region was varying according to gaze-direction induced eye opening, ranging from 1.4 cm for upward gaze to 0.8 cm for downward gaze). The monitor for these computer-presented images and the receiver faced each other at 100 cm distance, the ring of target objects placed midway between them. The computer screen and the receiver's chin-rest were adjusted to assure the same height for the sender's photograph's eyes, the receiver's eyes and the centre of the ring.

This setup closely reflected the one described under 2.3.1.: The computer-presented photographs of a sender gave gaze cues towards target locations, processing a randomly permuted list, while the human receiver tried to follow the gaze (indicated by the images' eyes) and to report its target. The slides showing static gaze of the sender towards the target were interleaved with images of the sender looking at the receiver's nasion for masking (see Fig. 2).

2.4. Definitions

The **deviation** (in degrees of visual angle) between the object gazed at by the sender and the object the receiver indicated was used for further analysis:

$$deviation = target(receiver) - target(sender) .$$

Overall, **accuracy** measures characterizing a condition were computed independently of the individual target position. They consisted of:

- **global precision** – the standard deviation of pooled deviations, called 'threshold' by Cline (1967), and

- **global bias** – the mean of pooled deviations. In case of a circular response target arrangement, this corresponds to a rotation between the actual target ring and the perceived ring of target locations.

These global measures were used to compare one condition to another.

Measures of **accuracy** of gaze following for individual sectors on the ring (as defined later in 2.5.2) were computed from trials in which the sender's gaze was aimed at neighbouring targets. They consisted of:

- **local precision** – the standard deviation of the pooled deviations of adjacent targets, and

- **local bias** – the mean of the deviations of adjacent targets (i.e., whithin a particular sector).

Thus, precision indicates the variation of receivers' answers and is a measure of dispersion, whereas bias is a measure of location. Low bias and high precision make up a high accuracy.

The local measures allowed us to calculate the precision of gaze following towards individual sectors, and to study whether there was a systematic bias depending on the target's position on the ring. Consequently, precision of the detection of a vertical displacement in gaze towards targets on the left and right side of the ring could be compared to each other as well as to the precision of the detection of a horizontal displacement in gaze towards targets on the upper and lower side, respectively (the target arrangement we used is depicted in Fig. 5 A, results section). More generally, the circular target arrangement allowed to assess any bias in a tangential direction to the target ring, and therewith the precision of target detection in all angular directions at a given eccentricity.

2.5. Data analysis

2.5.1. Comparison of conditions: global precision

For each of the five conditions detailed in 2.3., global precision and global bias were calculated across the twelve receivers. Within a condition, global precision specified the threshold of all receivers following gaze towards all target object locations. Global bias measured the tendency of the receivers to deviate either in clockwise direction (pos. values) or counter-clockwise (neg. values) on the target ring. It was tested against zero deviation using Student's t-test, $\alpha = 0.05$.

The global precision values of matching conditions were compared, and these pairs of conditions were statistically evaluated for a difference in response distributions using the two-sample Kolmogorov-Smirnov test, $\alpha = 0.05$ (see 3.1.).

2.5.2. Target position dependent (local) analysis

To study variation of gaze following accuracy (relative to individual target positions on the ring), local precision and local bias were calculated. Object positions were pooled into sectors to allow for statistical testing, which were

arranged as shown in Fig. 5 B. The arrangement of sectors allowed us to analyse displacements around the four cardinal half-axes. Therefore, two sectors of 5 object positions each were chosen for the vertical and two sectors of 6 object positions each for the horizontal half-axis. The quadrants in-between comprised 17 targets, divided into three sectors each. When local precision values for non-adjacent sectors were averaged (e.g., on the left and right side of the target ring), the square root of the mean of variances was calculated. Local bias for each of the 16 sectors was tested against zero deviation in 16 *t*-tests (α = 5% Bonferroni corrected); see 3.3.

Local bias can either be an effect relative to the local target configuration, or due to influences affecting a larger spatial field (e.g., a shift of the actual targets relative to the perceived targets in the frontoparallel plane). Such a large-area local bias might cause other forms of local bias (e.g., depending on the arrangement of adjacent objects) to be overlooked. Therefore, large-area influences were uncovered by filtering the deviations using a broad low-pass (Gaussian kernel, width 45 objects, FWHM 21 objects). By subtracting the filter result from the deviation data, i.e. adjusting for large-scale influences, regional local bias components were made visible; see 3.4.

2.5.3. Modelling of bias components

Several types of systematic bias can affect the relation between the actual target arrangement and the reports of a receiver. In our case, using a circular response target arrangement, all these offsets can be modelled in the plane perpendicular to the line of sight between sender and receiver (frontoparallel plane). Different target positions correspond to different spatial angles, analogous to a polar coordinate system, with the centre of the target ring as pole or origin. In our case, ϕ is the clockwise (seen from receiver's side) angle from the vertical ($=0°$) axis. All targets have the same radial distance, i.e. eccentricity, from the pole. Their position is defined by the angle ϕ (increasing

in steps of 4° per object on the target circle or 3.88° per degree of visual angle, in clockwise direction when seen from the receiver's side).

- If there is no bias, the identity function $\phi_{receiver} = \phi_{sender}$ relates the target perceived by the receiver to the object gazed at by the sender.

- For a global bias of an amplitude $\mathbf{g}$, i.e. when the mean of pooled deviations differs from zero, a rotation α with $\phi_{receiver} = \phi_{sender} + \alpha$ relates the actual target ring to the perceived ring of target locations ($\alpha = 3.88^{\circ} \cdot \mathbf{g}$). In naturalistic situations, this seems unlikely to occur.

- In case of a shift of the actual targets relative to the perceived targets in the frontoparallel plane, the radial distance to the pole remains the same, only $\phi_{receiver}$ changes in a nonlinear way. For a bias in upward direction (as we found), $\phi_{receiver}$ is smaller on the right side and larger on the left side of the setup, thus a bias of an amplitude $\mathbf{a}$ can be specified as $-\mathbf{a} \cdot \sin(\phi)$. Then, the function relating the perceived target to the position gazed at is given by

$$\phi_{receiver} = \phi_{sender} - \mathbf{a} \cdot \sin(\phi_{sender})$$

- A tendency to deviate towards the four cardinal half-axes, out of the sectors at the diagonals, can be specified as $-\mathbf{b} \cdot \sin(4 \cdot \phi)$. See Fig. 7 A for a visualisation. If this occurs in addition to an upward bias $\mathbf{a}$, the equation for the combined relation is

$$\phi_{receiver} = \phi_{sender} - \mathbf{a} \cdot \sin(\phi_{sender}) - \mathbf{b} \cdot \sin(4 \cdot \phi_{sender})$$

The amplitude of $\mathbf{a}$ and $\mathbf{b}$ was estimated by fitting the model function to the data (MATLAB release 13, The MathWorks, Inc., curve fitting toolbox) as shown in Fig. 7 B.

3. Results

In our setup (target objects at an eccentricity of 15° visual angle with a spacing of 1.03°), receivers perceived the true target in 14% of 7560 trials (pooled over all subjects and conditions), and normally distributed deviations ranging from $-12.4°$ to $+12.4°$ were observed. For all five conditions (see 2.3.) pooled, global precision was 3.17° visual angle with a global bias of 0.04°. In other words, two thirds of the receivers' responses deviated less than three object positions from the target gazed at by the sender.

3.1. Comparison of conditions: global precision

Histograms of the deviation distributions obtained under the five different conditions detailed in 2.3. are shown in Fig. 3. The following global precision and global bias were observed:

A) In the 'dynamic' condition, where the receiver followed the sender's saccade in binocular vision, global precision was highest with **2.81**° visual angle, and no significant global bias was observed (bias −0.08°, p=0.32).

B) In the 'static' condition, where the target was defined by static gaze in binocular vision, global precision was **3.09**° visual angle, and no significant global bias was observed (bias −0.12°, p=0.20).

C) In the 'receiver monocular' condition, using static gaze of the sender with one eye of the receiver occluded, a global precision of **2.97**° visual angle and a global bias of 0.13° were observed (p=0.04).

D) In the 'sender monocular' condition, using static gaze of the sender with one eye masked, global precision was **3.62**° visual angle, and no significant global bias was observed (bias −0.05°, p=0.52).

E) In the ‘computer sender’ condition, where photographic images replaced the natural sender (for a binocular receiver), a global precision of **2.97**° visual angle and a global bias of 0.34° were observed (p<0.01). When interviewed for their subjective impression, receivers reported the gaze of the sender to be dynamically alternating between eye contact and target.

These conditions were compared for a difference in distributions using the two sample Kolmogorov-Smirnov test:

a) Global precision seemed to be slightly higher in the ‘dynamic’ (A) than in the ‘static’ (B) condition. However, the difference did not reach statistical significance (p = 0.41). Hence, the role of dynamic vision of eye movements in gaze following does not seem to be prominent.

b) Monocular vision of the receiver (‘receiver monocular’ condition, C) was not significantly different from binocular vision in the ‘static’ (B) condition (p = 0.11). Therefore, binocular disparity cues seem to be dispensable for the extraction of gaze direction.

c) On the other hand, receivers were less accurate if one eye of the sender was masked (‘sender monocular’ condition, D) than when both eyes were visible in the ‘static’ (B) condition, and both distributions differed significantly (p<0.03). Gaze position information derived from both eyes appears to be integrated.

d) Finally, global precision for following the gaze of computer-presented photographic images (‘computer sender’ condition, see 2.3. E) was similar to that obtained when following the gaze of a natural sender (‘dynamic’ condition, 2.3. A). However, the distributions differed significantly ($p < 0.01$) because of a difference in global bias, not global precision. The ‘computer sender’ condition (2.3. E) featured a global bias significantly different from

zero. This might be due to an artefact in image presentation, i.e. an alignment problem between digital camera and computer screen, corresponding to 1.32° angle of rotation as described in 4.1. The comparison was carried out against the 'dynamic' condition (2.3. A) because, in a standardised questionnaire after the experiment, receivers unanimously reported they 'felt that the eye moved', possibly caused by the mask images interleaved into the presentation (see 2.3.2.).

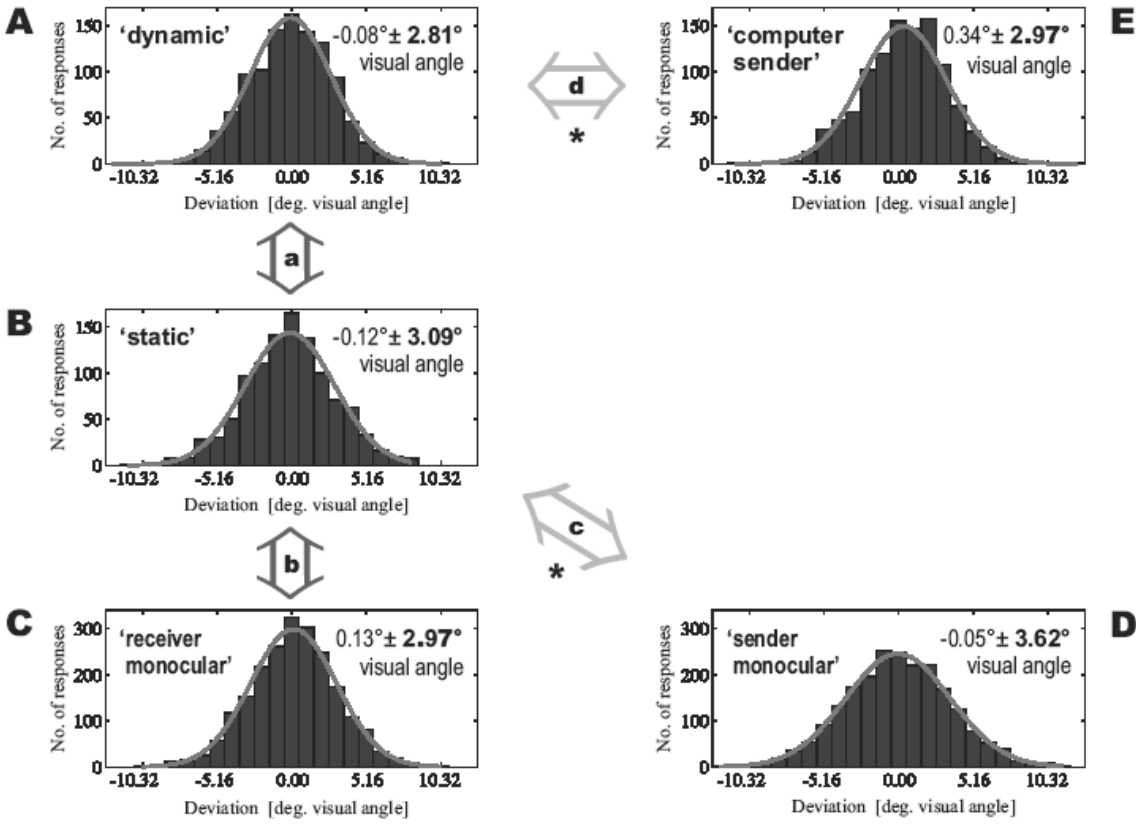

Fig. 3. Variation of gaze following precision between the different conditions, A) the receiver following the sender's saccade in binocular vision, B) the target defined by static gaze in binocular vision, C) monocular vision on the receiver's side for static sender's gaze, D) monocular visibility on the sender's side for static sender's gaze and E) computer-presented photographic images replacing the sender (difference due to bias, not precision; see 3.1. d). The maximum likelihood fit of a normal distribution is superimposed on each histogram, and precision is indicated as 'global bias ± global precision'. ∗ , $p < 0.05$.

3.2. Local precision anisotropy

Examination of the distribution of targets reported by the receivers pooled over subjects and conditions revealed a clear deviation from uniformity. The numbers of targets located close to the cardinal half-axes at the left, right, upper and lower side of the ring were given more frequently (see Fig. 4 A).

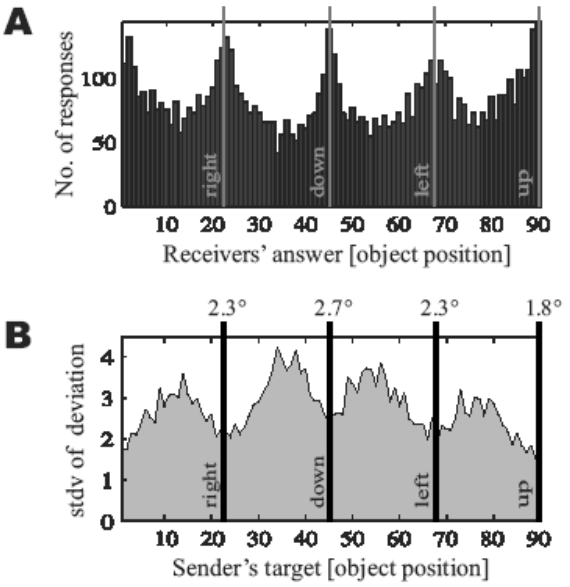

Fig. 4. A) Receivers answers cumulated for numbers of targets from the left, right, upper and lower side of the ring. B) Local precision was increased for following gaze towards targets around the horizontal and vertical axis, averaging to the values indicated above the bars. See Fig. 5 A for local bias.

Furthermore, local precision varied in an angle dependent manner around the ring: good precision for detecting gaze towards targets around the horizontal and vertical axis and somewhat worse precision for the diagonals, as shown in Fig. 4 B. Local precision was calculated for sectors of pooled responses towards adjacent targets, as described under 2.5.2. Local precision was best for the topmost sector (1.8° visual angle), followed by the two sectors around the horizontal axis (2.3°, each) and the sector at the bottom of the ring (2.7°). Mean precision for these four sectors around the horizontal and vertical axis was 2.3° visual angle. Local precision for the sectors containing the diagonals was somewhat worse (2.9° top left, 3.1° top right, 3.6° bottom left and 3.9° bottom right), averaging to 3.4° visual angle. Thus, mean precision was diminished by a factor of 1.48 for the sectors around the diagonals.

3.3. Upward bias

Receivers were biased to deviate in an upward direction. Whereas local precision was good for any of the four cardinal half-axes, only the two vertical half-axes were characterized by an absence of a significant local response bias. As suggested in Fig. 5 A, which plots the local bias as function of target position, subjects displayed an upward bias for gaze towards targets on the left and right side of the ring:

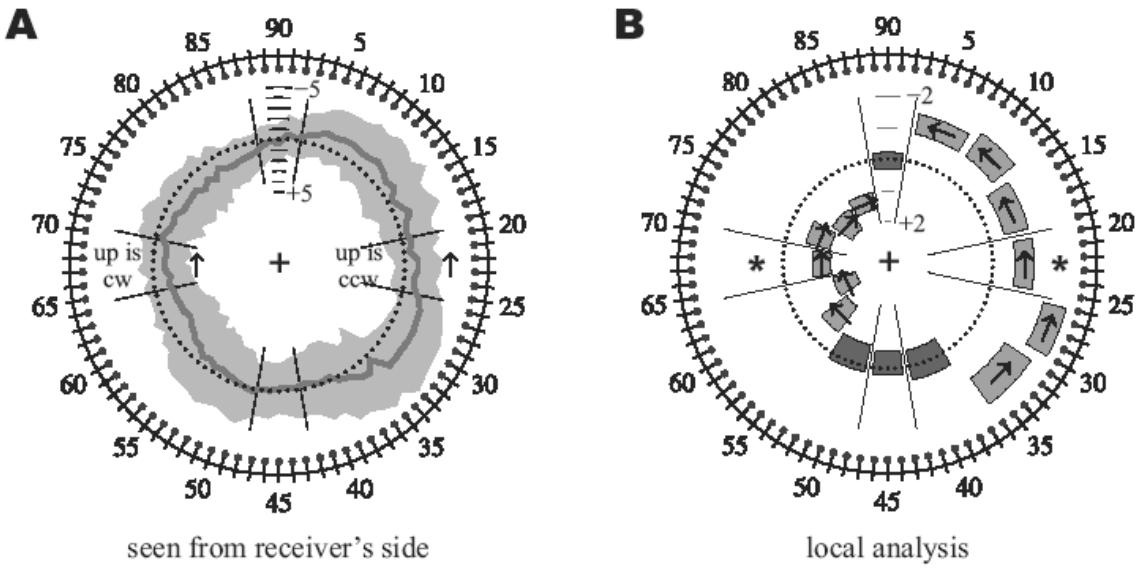

Fig. 5. Upward bias for targets on the left and right side of the setup. Outer ring depicts the object configuration as seen by receivers (90 pinhead targets), inner ring raw deviation data (A) and analysed local bias (B), pooled over subjects and conditions, relative to true target position (dotted line). Low eccentricity stands for clockwise (cw) or pos. deviation, high eccentricity for counterclockwise (ccw) or neg. deviation. Local bias (thick line) ± local precision (shaded band). Confidence intervals (CI) of t-tests on local bias. Length: targets pooled (see 2.5.2.), width: CI width, ↑: p<0.05 Bonferroni corrected. *: upward bias of 1.3° visual angle on the left and 1.1° on the right side.

- On the left side (objects 65 to 70), receivers reported larger object numbers than the sender had looked at. Hence their deviation on the left side had an upward direction, and local bias was positive (Fig. 5 A: centripetal to the dotted ‘no bias’ line, indicating a clockwise shift on the ring).

- On the right side (objects 20 to 25), receivers reported smaller object numbers than the sender had looked at. Hence their deviation on the right side also had an upward direction, and local bias was negative (Fig. 5 A: centrifugal to the dotted ‘no bias’ line, indicating a counterclockwise shift on the ring).

The significance of the local bias suggested by this raw plot, pooled over subjects and conditions, was assessed in the following manner: To achieve larger, gaussian shaped distributions for subsequent t-tests, data for adjacent targets was further pooled into 16 sectors across the setup ring, as described under 2.5.2.. Deviation distributions for these sectors were tested against ‘no bias’, resulting in Fig. 5 B. Sector length shows the number of target locations pooled, sector width gives the lower (higher eccentricity) and upper (lower eccentricity) confidence interval bounds. The direction of all significant deviations is indicated by arrows superimposed on the sectors. For all sectors on the left and right side of the setup, local bias was consistent with a significant deviation in upward direction. This effect was consistently found when analysing the individual conditions and subjects’ data, although due to the smaller distribution size in unpooled data not all sectors reached significance. Upward bias at the left cardinal half-axis amounted to 1.3° visual angle, at the right one to 1.1° (corresponding to a skew larger than the distance between two target objects).

3.4. Cardinal-axis bias

There is more than upward bias: local bias relative to the cardinal axes. An upward shift in perception of gaze towards targets in the frontoparallel plane

(*upward bias*) affects large parts of the target zone, which might conceal other forms of local bias (e.g., relative to certain target positions on the ring and thus depending on the arrangement of adjacent objects). This is why we tried to remove the influence of the upward bias by estimating its influence using low-pass filtering of the raw data and subtracting the filter output from the raw data (as described under 2.5.2.). Raw deviation data, in relation to large-area upward bias and deviations corrected for upward bias, are shown in Fig. 6 A. Re-evaluation of deviations corrected for the upward bias is displayed in Fig. 6 B (subjected to the same analysis as done for Fig. 5 B, previous section). That our attempt to remove the influence of the upward bias was successful is indicated by the fact that the corrected local bias for the sectors at the left and right cardinal half-axes did no longer deviate significantly from the true target position.

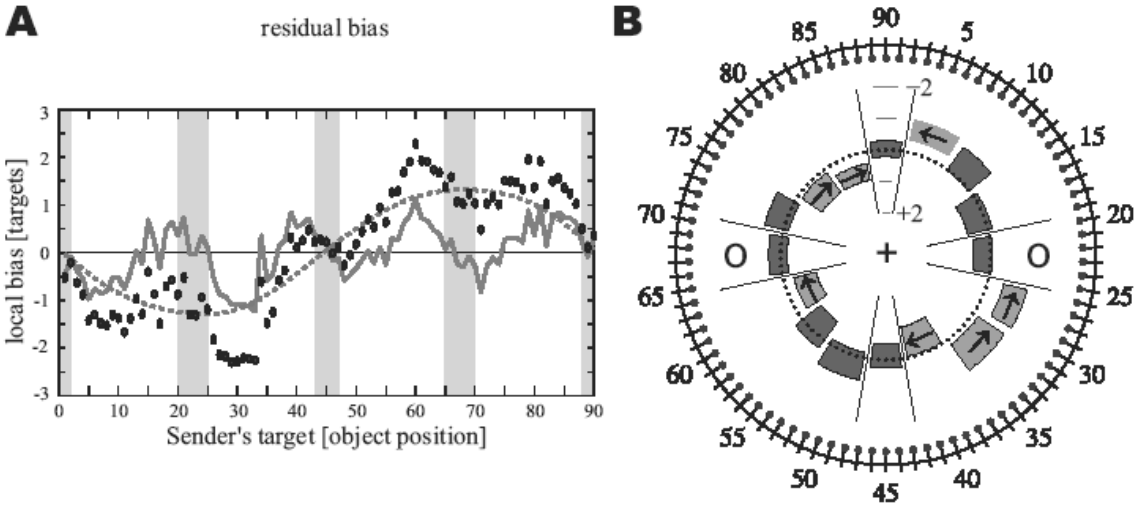

Fig. 6. Cardinal-axis bias: local bias remaining after eliminating the upward bias.

A) Linearised plot of raw deviation data (•), low-pass filtered deviation data (dotted line; 'upward bias'), and deviations after subtraction of the low-pass filtered deviation data (thick line), against true target position (thin line at zero). Bars indicate the sectors at the cardinal half-axes.

B) Outer ring: object configuration as seen by receivers, inner ring: confidence intervals (CI) of t-tests on residual deviations for adjacent

targets, relative to true target position (dotted line). Length: targets pooled, width: CI width, ↑: p<0.05, plotted as in Fig. 5 B.

After the upward bias has been removed (sectors ◦), a remaining local bias towards the cardinal axes stands out: receivers tend to deviate away from the diagonals. However, significant residual local bias was found in seven of the twelve sectors in the quadrants located at the diagonals, pointing towards the cardinal axes. In addition, the plot of deviations corrected for upward bias (Fig. 6 A, thick line) showed zero-crossings at the four cardinal half-axes always to occur from positive to negative deviation values, whereas at target positions representing the diagonals in-between, zero-crossing occurred from negative to positive deviation values. This is equivalent to a skew towards the cardinal axes, away from the diagonals. These findings for residual local *bias* data are in line with the results for local *precision* anisotropy, where targets located around the cardinal axes were reported more frequently (Fig. 4 A), and mean local precision for sectors at the diagonals was 48% inferior to local precision for sectors at the cardinal axes (Fig. 4 B). Thus, in addition to the upward bias, a *cardinal-axis bias* was observed, indicating that receivers tend to deviate towards these particular locations. Further work needs to be done to show whether the cardinal axes are special due to characteristics of the sender's faces, due to being horizontally and vertically aligned in world coordinates or due to their orientation with respect to the receiver's body.

3.5. Estimates obtained by modelling local bias and local precision

When expressed in a polar coordinate system, an upward shift is given by a sine wave of an angular frequency of one per period (i.e. full cycle around the ring), and a shift towards the cardinal axes by a sine wave of an angular frequency of four per period (see 2.5.3. and Fig. 7 A). Therefore, parameters of the model curve can be estimated by fitting it to the deviation data. Fig. 7 B shows the relation between raw deviation data, the model function for upward bias and the model function for combined upward bias and cardinal-axis bias.

The amplitude $\mathbf{a}$ of the upward bias was estimated to be $\mathbf{a} = 1.67^\circ$ visual angle ($r^2 = 0.805$, 95% confidence bounds 1.50° and 1.84°) by a least squares fit of the model function for upward bias to the deviations pooled over subjects and conditions. Regression analysis of combined upward bias and cardinal-axis bias revealed an upward bias of $\mathbf{a} = 1.67^\circ$ (95% confidence bounds 1.55° and 1.78°) and a cardinal-axis bias of $\mathbf{b} = 0.61^\circ$ (95% confidence bounds 0.49° and 0.72°) with a $r^2 = 0.91$.

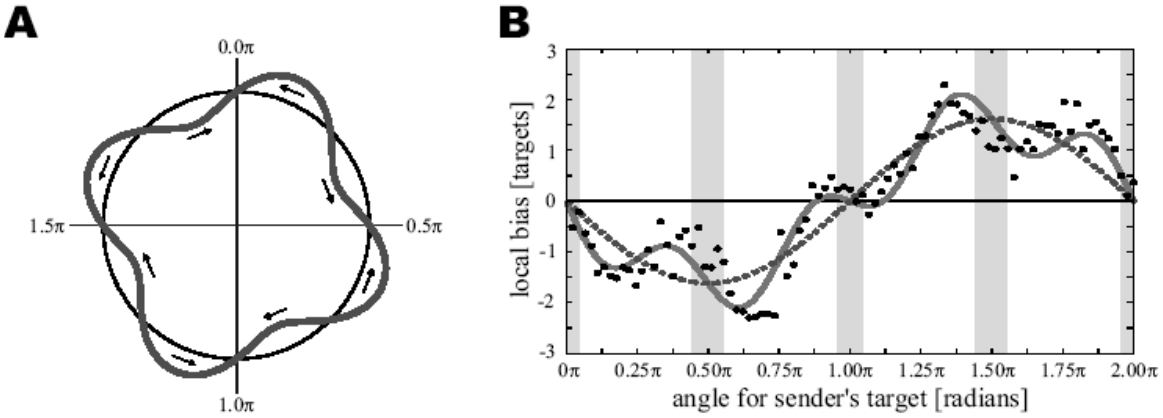

Fig. 7. Model of cardinal-axis bias.

A) Model plot of a skew towards the four cardinal half-axes, away from the diagonals. $\phi_{thick.line} = \phi_{thin.line} - \sin(4 \cdot \phi_{thin.line})$**.**

B) Raw deviation data pooled over subjects and conditions (•), overlaid with a model plot for upward bias $\phi_{receiver} = \phi_{sender} - \mathbf{a} \cdot \sin(\phi_{sender})$ **(dotted line,** $r^2 = 0.805$**) and a model plot for combined upward and cardinal-axis bias** $\phi_{receiver} = \phi_{sender} - \mathbf{a} \cdot \sin(\phi_{sender}) - \mathbf{b} \cdot \sin(4 \cdot \phi_{sender})$ **(thick line,** $r^2 = 0.91$**), against true target position (thin line). Bars indicate the sectors at the cardinal half-axes.** $\mathbf{a} = 1.67^\circ$ **visual angle,** $\mathbf{b} = 0.61^\circ$**.**

4. Discussion

We investigated the capability of a *receiver* to direct his eye-gaze to an *object* singled out of an array of identical objects by the eye-gaze of a *sender*. The accuracy of this triadic gaze following was compared under conditions manipulating the receiver's vision as well as the sender cues available for guiding the receiver's eyes. ***Global precision*** ranging from 2.81° visual angle (best performance for dynamic vision of sender's saccade) to 3.62° (receiver limited to see only one of the sender's eyes) was observed. The circular arrangement of response targets used in our experimental system allowed us to study gaze towards objects positioned at all spatial angles with respect to the sender's eyes, measuring precision for horizontal, vertical as well as diagonal offsets, within the same session. Indeed, ***local precision*** varied depending on the target position, ranging from 1.8° for the best to 3.9° for the worst sector of adjacent target positions. Its anisotropic distribution favoured the four sectors at the cardinal half-axes (mean precision 2.3°) against the four sectors at the diagonals (mean precision 3.4°), and the top sector (1.8°) against the bottom sector (2.7°). Not only local *precision*, but also ***local bias*** indicated a striking anisotropy. On average, targets within the left and right sector were reported more than one position higher than they actually were: *upward bias*. In addition, reports were skewed towards the horizontal and vertical axes: *cardinal-axis bias*.

4.1. Comparison of global precision to previous studies

Other studies investigated gaze following in a quantitative manner, some of them mainly in terms of dyadic gaze (Gibson & Pick, 1963; Cline, 1967; Anstis et al., 1969; Masame, 1990; Symons et al., 2004; Poppe, Rienks, & Heylen, 2006). Triadic gaze is more complex than dyadic gaze in that it involves a third party as the focus of attention of sender and receiver. In dyadic eye-gaze, it might be sufficient to detect mirror symmetry of the two eyes (sender's head facing the receiver), whereas in triadic eye-gaze presumably the direction of the

eyes has to be triangulated with the positions of two persons and an object in space. The present setup focused on frontal orientation of the sender's and receiver's head. The situation is different when the sender's head is turned to one side as in the known "Mona Lisa" gaze (Todorović, 2006). In this case, there might be no complexity difference between dyadic and triadic gaze.

The first study by Gibson & Pick (1963) examined purely *dyadic* interaction: Their receivers judged whether a sender looked at them, while the sender's gaze was directed towards either the receiver's nasion, or horizontally displaced. Precision, termed threshold, was 2.8° visual angle (standard deviation of the responses for which the receiver felt being looked at). Cline (1967) used sender's targets arranged in cross-hair fashion, invisible to the receiver who gave responses by pointing to locations on a transparent response board. For the centre (i.e., mutual gaze) he reported a somewhat better precision of 0.7° visual angle horizontally and 1.3° visual angle vertically. Thus, in both studies, precision for detecting direct gaze was better than the global precision we obtained at 15° eccentricity. Cline found judgements of gaze towards off-centre targets (8° and 12° eccentricity) to be significantly less accurate, averaging to 3.1°, which was within a similar range as our results. Anstis et al. (1969) computed a linear regression relating the actual to the perceived direction of gaze. Both Cline's and Anstis' work was based on a sender attending to a virtual target not visible to the receiver. This constituted a triadic situation for the sender, but no *joint visual attention* between sender and receiver. *Triadic* gaze was studied in recent work by Symons et al. (2004), with target objects arranged on a horizontal bar considerably below the line of eye contact. Therefore, the eccentricity of their target object from the line of eye contact varied in a nonlinear way, depending on the position on the horizontal bar. The setups of Anstis et al. (1969) and Symons et al. (2004) have to deal with local distortions caused by the endings of a finite linear bar. Because Symons et al. (2004) used a two alternative forced choice task (whether the sender was looking left or right of a given target), they applied a standard psychophysical function for analysis, which necessitated different target

distances for different conditions and prevented the analysis of local bias components. Thus, although they compared similar conditions as we did, no quantitative relation of their values to ours can be given, but their results seem to be in agreement with ours:

a) The role of dynamic vision of the movement of the eye does not seem to be prominent in gaze following: Like Symons et al. (2004), we observed no significant differences between the receiver using dynamic vision or the sender's static gaze towards a target.

b) Binocular disparity cues do not contribute to precision: Receivers using monocular vision were as precise as receivers allowed to use binocular vision.

c) Information derived from both sender's eyes is integrated: Like Symons et al. (2004), we found a significant decline of acuity if one of the sender's eyes was masked.

d) It seems to be feasible to use computer-presented photographic images instead of a natural sender, although there might be pitfalls in generating them: Global precision for following the gaze of images was similar to that obtained for a natural sender, although the deviation distributions differed significantly -because of a difference in global bias. The 'computer sender' condition (Fig. 3 E) featured the largest global bias, significantly different from zero, probably due to an artefact in image presentation. The digital camera and the computer screen might have been slightly rotated against each other, by 1.32° corresponding to 0.34° visual angle. Symons et al. (2004) also obtained a qualitatively comparable result when they replaced their natural sender by computer-presented photographs. The quantitative difference might be due to the fact that in their setup, the size of the sender's head (eye base) and the distance to the objects varied from the natural sender condition. We chose to compare the 'computer sender' to dynamic vision because receivers unanimously reported they 'felt that the eye

moved', possibly caused by the mask images interleaved into the presentation. We observed a precision value in-between the one found for dynamic and static vision.

A computer controlled sender has several advantages (for example, no change in facial expressions, no influence of the receiver's actions on the sender, exact repetition of the gaze towards each target position), and in some cases such as functional imaging studies it might be the only option. Using a photograph adds the possibility to manipulate the image as well as the timing of the presentation. However, great care has to be taken when generating the image to be able to obtain quantitative, not only qualitative, information.

4.2. Local precision anisotropy is in line with previous studies

For positions at 8° and 12° eccentricity (no target visible to the receiver), Cline (1967) observed a mean precision at the horizontal axis of 3.2° horizontally and 2.9° vertically. For positions at the vertical axis, precision was 2.4° horizontally and 3.8° vertically. This corresponds to our results at 15° eccentricity, which show a slightly better local precision, 2.3° both for the sectors at the two horizontal half-axes (vertically) and for the sectors at the two vertical half-axes (horizontally). Anstis et al. (1969) found that their receivers overestimated the eccentricity of the sender's gaze systematically by 50% for targets on the horizontal axis, whereas no such bias was found for targets on the vertical axis. Horizontal overestimation is congruent with studies of Cline (1967) and Symons et al. (2004), but Cline observed overestimation for vertical eccentricities, as well. Masame (1990), who replicated the study of Anstis et al. (1969), found an underestimation of gaze direction for gazes closer to or at the ears of the sender, in addition to an overestimation for gaze at wider angles. Anstis et al. (1969) argued that the overestimation would be due to the partial covering of the eyeball within the orbit, which they tested by using an artificial eyeball (visible through the hole in a diaphragm) as 'sender', and observed that the overestimation was smaller for a larger hole. They concluded that

judgements of direction of gaze were determined principally by the position of the pupil in the visible part of the eye.

In the previous setups, the only possible bias observed was a compression or expansion of gaze direction distances in regard to the centre of the target scale – they were limited to radial bias components. In contrast, our setup allowed to measure triadic gaze following towards objects at all spatial angles with respect to the line of eye contact between sender and receiver. In particular, horizontal and vertical bias components could be quantitatively compared since they were measured in the same experiment. However, we are aware of the limitation that we could only detect bias components tangential to the ring of target objects. The only setup to investigate radial as well as frontoparallel bias components would be a plane of objects perpendicular to the line of eye contact between sender and receiver.

4.3. Receivers' bias in upward direction

Although receivers showed the second highest local precision for gaze towards targets at the left and right side of the setup, they reported their position to be more than one object higher than it actually was, on average skewed upward by 1.2°. Cline (1967) also observed an upward bias, for all targets at the level of the eyes or higher, averaging to 2.2° for targets on the horizontal axis. Hence Cline's upward bias was even larger than ours, but was only found for targets above the line of eye contact. However, the unexpected deviation we found suggests an upward shift in the perception of gaze towards all targets in the frontoparallel plane. Our setup allowed us to measure deviations directed tangentially to the ring, but we observed an upward bias only for the left and right side of the setup (Fig. 5 B). Assuming a simple model function for the upward bias (see 2.5.3.), 80% of the variance of the deviations could be explained (Fig. 7 B). The top and bottom sector were reported accurately, although they differed in local precision, which was considerably better for the top (1.8°) than for the bottom sector (2.7°). An explanation for this difference

might be the upward bias itself, since, on a ring, an upward shift disperses objects at the bottom while accumulating objects at the top. In fact, mean precision for the top and bottom sector, 2.3°, was the same as found in the left and right sectors.

While the upward bias was significant, and consistently observed in pooled data as well as in the different conditions, its origin remains unknown. In case the bias is caused by an anisotropy in the receiver system (one of the three possibilities discussed in 4.5., and most likely concerning the receiver's percept), it may be plausible to relate it to one of the well-established vertical asymmetries in the patterns of eye movements. It is typical for memory-guided saccades (performed in darkness towards a remembered location) to display an upward shift in the endpoints (Gnadt, Bracewell, & Andersen, 1991; White, Sparks, & Stanford, 1994; Barton & Sparks, 2001), although this effect seems to be more prominent in monkeys than in humans. Macaque monkeys demonstrate an upward offset when fixating in the dark, which may be due to the nonuniform distribution of rods in the retina (Barash, Melikyan, Sivakov, & Tauber, 1998). Attentional resolution was found to be better in the lower than in the upper visual field (He, Cavanagh, & Intriligator, 1996), which might be an incentive to diverge slightly from the target. Upward bias has also been found in the gain of the vestibuloocular and optokinetic reflex, which has been attributed to a gravity-dependent asymmetry (Vogelstein, Snyder, & Angelaki, 2003).

4.4. Receivers' bias towards the cardinal axes

It was plausible to search for a systematic bias in relation to the cardinal axes, because targets located around the cardinal axes were reported more frequently (Fig. 4 A), and mean local precision for sectors at the diagonals was 48% inferior than local precision for sectors centered on the cardinal axes (Fig. 4 B). Both could be explained by a *cardinal-axis bias*, a tendency of receivers to deviate towards the horizontal and vertical sectors (Fig. 7 A). In this case, the sectors at the four cardinal half-axes not only would have to show high local

precision, but responses needed to be accurate as well. However, only the two sectors on the vertical axis were free of a local bias. This inaccuracy was due to the upward bias for the two sectors on the horizontal axis. When the upward bias was removed from the deviation data, the sectors on the left and right cardinal half-axes were accurate, indicating that all their deviation had been fully accounted for by the upward bias (Fig. 6 B). A remaining local bias was significant in seven of the twelve sectors around the diagonals, mainly pointing towards the cardinal axes. In addition, the plot of deviations corrected for upward bias (Fig. 6 A, thick line) showed zero-crossings at the four cardinal half-axes, always occurring from positive to negative deviation values, whereas at target positions representing the diagonals, zero-crossing occurred from negative to positive deviation values. This is equivalent to the expected skew towards the cardinal axes, away from the diagonals. By integrating cardinal-axis bias into the model function for upward bias, 91% of the variance of the deviations could be explained (Fig. 7 B).

In case the cardinal axes are special due to their clear orientation with respect to the receiver's body, it is plausible to relate the cardinal-axis bias to the motor aspects of gaze following, namely that horizontal and vertical saccades are generated by separate populations of premotor neurons (Becker & Jürgens, 1990; Leigh & Kennard, 2004). However, orientation-selective mechanisms have also been reported in visual perception (Foster, Savage, Mannan, & Ruddock, 2000), although little is known how they might influence the perceptual properties of gaze following. Thus, further work is needed to identify the frame of reference for gaze following, which might allow an insight to be gained into the underlying neural circuitry, as discussed in the next section.

4.5. In which frame of reference is gaze following coded?

Analysis of the anisotropy of local precision and local bias might tell us more about the processes involved in perception and action of a person following the gaze of another. The orientation of local bias in respect to external and internal

influences is of special interest, since knowledge of the frame of reference in which gaze following is coded (‘sender-centric’, allocentric or ‘receiver-centric’) might narrow down the range of sensorimotor modules involved in it.

‘sender-centric’: The gaze direction perceived by the receiver might be influenced by symmetries in the sender’s face and eye cues such as the amount of scleral whiteness at each side of the iris, or the position of the iris or pupil in the visible part of the eye (Anstis et al., 1969). In this case, gaze following should be coded *‘sender-centric’*. Our finding of an increased global precision if both eyes of the sender were visible supports this hypothesis. However, we did not find a difference in local precision between sectors horizontally and vertically displaced from the line of eye contact. This would be expected in a sender-centric analysis, since local symmetry can be used for detecting the horizontal displacements at the vertical axis only (face: both eyes mirrored at the nose; eye: same amount of scleral whiteness on both sides of the iris). As shown in Fig. 2, the position of the iris and pupil within the eye of the sender indeed displays an anisotropy depending on his direction of gaze on the target ring. A striking feature is the correlation between the vertical extent of the eye openings and the vertical position of the target, which can explain the poorer local precision for the lower half of the targets (see Fig. 4 B), due to partial occlusion of iris and pupil. In the interpretation of the upward bias a feature like the vertical extent of the eye opening is unlikely to be involved, since this bias is similar for the upper and lower half of the targets. A sender-centric explanation of the cardinal-axis bias is hindered by the influence of the vertical extent of the eye opening on the symmetry axes of the eye. At least, the potential effect on horizontal displacements (by local symmetry) and on vertical displacements (possibly by comparing the height of the target to the height of the straight line through both sender’s eyes) should be different. The points discussed above emphasize *geometrical* cues. However, there is cumulating evidence for non-geometric cues: Ricciardelli, Baylis, & Driver (2000) demonstrate that gaze following is disrupted by a reversed contrast polarity of the sender’s eye (black sclera and white pupil, preserving the geometric

properties). Ando (2002) shows in dyadic eye-gaze that reducing scleral brightness on one side of the iris in photographs of a sender results in a shift of the perceived direction of gaze towards the darkened side of the eye.

allocentric: Our demonstration of a cardinal-axis bias may prompt to postulate an *allocentric* or 'world centered' coding of gaze following, for example linking the horizontal axis to the horizon and the vertical axis to gravity. In the case of uncertainties in the judgement of gaze, receivers might prefer these exceptional directions.

'receiver-centric': In case of an 'action based' analysis of eye gaze, the receiver would mimick the saccade of the sender, and find its target by looking at it himself instead of triangulating a gaze path. This would require gaze following to be coded *'receiver-centric'*. In everyday life, the most relevant out of several targets is often selected after following gaze at the general location. Vertical target displacements (horizontal axis) might be easier to detect at eye height. In naturalistic situations, perception and action often appear to be coupled (e.g., grasping tasks or posture control). However, we found no significant difference in global precision between the 'dynamic' and 'static' condition (with and without sender's saccade). The effect of mimicking itself may be tested by using another means of receiver's report while maintaining fixation to the sender's nasion (e.g., pointing towards targets or indicating their coordinates).

Further work is needed to clarify whether gaze following is coded relative to the body of the sender, or of the receiver, or in allocentric coordinates. This can be done by investigating the effect of rotating either the sender's face, the receiver, or both, around their line of eye contact. The direction of an upward bias, as well as the axes of a cardinal-axis bias, should rotate with the respective frame of reference it depends on.

5. Conclusion

The present study provides a convenient experimental system which allowed us to investigate triadic gaze following towards objects at all spatial angles with respect to the line of eye contact between sender and receiver. Due to a circular arrangement of response targets, our setup allowed us, for the first time, to measure precision for horizontal and vertical as well as diagonal offsets. Therefore, target object configuration (such as the orientation of, or endings of a linear bar) could not influence receivers' performance. The results suggest that human gaze following is very precise in general. It is also surprisingly robust to manipulations of the sender cues available for guiding the receiver's eyes, as long as both eyes of the sender are visible. The present study demonstrates that binocular disparity cues are not used for eye-gaze following. In addition, it shows the feasibility of utilising computer-presented images as sender in gaze following studies.

Accuracy was increased for positions left, right, above and below of the eyes being followed. Furthermore, two types of systematic bias could be identified: *Upward bias* (receivers' percept of a sender's gaze being directed towards an object above the actual target) and *cardinal-axis bias* (receivers' perceiving the sender's gaze to be directed towards positions left, right, above and below of the line of eye contact even if the actual target was located closer to a diagonal). Further work is needed to clarify the origins and role of both types of bias. This is important because it might lead to knowledge of the frame of reference ('sender-centric', allocentric or 'receiver-centric') used in gaze following, helping to narrow down the range of sensorimotor modules involved, thereby facilitating the search for its neural correlates.

6. Acknowledgements

We thank Dr. Christine Bock, née Falch, for valuable suggestions. This project was supported by BMBF grant 01GA0503.

References

Ando, S., (2002). Luminance-induced shift in the apparent direction of gaze., *Perception*, 31 (6) 657–674.

Anstis, S. M., Mayhew, J. W., & Morley, T. (1969). The perception of where a face or television “portrait” is looking. *Am J Psychol*, 82(4):474–489.

Barash, S., Melikyan, A., Sivakov, A., & Tauber, M. (1998). Shift of visual fixation dependent on background illumination. *J Neurophysiol*, 79(5):2766–2781.

Baron-Cohen, S. (1994). How to build a baby that can read minds: Cognitive mechanisms in mindreading. *Cahiers de Psychologie Cognitive / Current Psychology of Cognition*, 13:513–552.

Barton, E. J. & Sparks, D. L. (2001). Saccades to remembered targets exhibit enhanced orbital position effects in monkeys. *Vision Res*, 41(18):2393–2406.

Becker, W. & Jürgens, R. (1990). Human oblique saccades: quantitative analysis of the relation between horizontal and vertical components. *Vision Res*, 30(6):893–920.

Butterworth, G. (1991). The ontogeny and phylogeny of joint visual attention. In Whiten, A., editor, *Natural theories of mind: Evolution, development, and simulation of everyday mindreading*, pages 223–232, Oxford, England. Blackwell.

Cline, M. G. (1967). The perception of where a person is looking. *Am J Psychol*, 80(1):41–50.

Dalton, K. M., Nacewicz, B. M., Johnstone, T., Schaefer, H. S., Gernsbacher, M. A., Goldsmith, H. H., Alexander, A. L., & Davidson, R. J. (2005). Gaze fixation and the neural circuitry of face processing in autism. *Nat Neurosci*, 8(4):519–526.

Emery, N. J. (2000). The eyes have it: the neuroethology, function and evolution of social gaze. *Neurosci Biobehav Rev*, 24(6):581–604.

Farroni, T., Csibra, G., Simion, F., & Johnson, M. H. (2002). Eye contact detection in humans from birth. *Proc Natl Acad Sci U S A*, 99(14):9602–9605.

Foster, D. H., Savage, C. J., Mannan, S., & Ruddock, K. H. (2000). Asymmetries of saccadic eye movements in oriented-line-target search. *Vision Res*, 40(1):65–70.

Gibson, J. J. & Pick, A. D. (1963). Perception of another person's looking behavior. *Am J Psychol*, 76:386–394.

Gnadt, J. W., Bracewell, R. M., & Andersen, R. A. (1991). Sensorimotor transformation during eye movements to remembered visual targets. *Vision Res*, 31(4):693–715.

He, S., Cavanagh, P., & Intriligator, J. (1996). Attentional resolution and the locus of visual awareness. *Nature*, 383(6598):334–337.

Kampe, K. K., Frith, C. D., Dolan, R. J., & Frith, U. (2001). Reward value of attractiveness and gaze. *Nature*, 413(6856):589.

Leigh, R. J. & Kennard, C. (2004). Using saccades as a research tool in the clinical neurosciences. *Brain*, 127(Pt 3):460–477.

Masame, K. (1990). Perception where a person is looking: overestimation and underestimation of gaze direction. *Tohoku Psychologica Folia*, 49, 33-41.

Poppe, R., Rienks, R., & Heylen, D. (2007). Accuracy of head orientation perception in triadic situations: Experiment in a virtual environment. *Perception*, 36, 971-979.

Ricciardelli, P., Baylis, G., Driver, J. (2000). The positive and negative of human expertise in gaze perception., *Cognition*, 77 (1) B1–14.

Symons, L. A., Lee, K., Cedrone, C. C., & Nishimura, M. (2004). What are you looking at? Acuity for triadic eye gaze. *J Gen Psychol*, 131(4):451–469.

Todorović, D. (2006). Geometrical basis of perception of gaze direction. *Vision Res*, 46, 3549-3562.

Vogelstein, J. T., Snyder, L. H., & Angelaki, D. E. (2003). Accuracy of saccades to remembered targets as a function of body orientation in space. *J Neurophysiol*, 90(1):521–524.

Wada, J. A. (1961). Modification of cortically induced responses in brain stem by shift of attention in monkeys. *Science*, 133:40–42.

White, J. M., Sparks, D. L., & Stanford, T. R. (1994). Saccades to remembered target locations: an analysis of systematic and variable errors. *Vision Res*, 34(1):79–92.

Lebenslauf

Persönliche Daten

Name	SIMON WALTER BOCK
Geburtsdatum	10. 9. 1974
Geburtsort	Tübingen
Familienstand	verheiratet
Staatsangehörigkeit	deutsch

Schule

1981 – 1987	Grundschule und Orientierungsstufe in Göttingen
1987 – 1989	Max-Planck-Gymnasium in Göttingen
1989 – 1994	Uhland-Gymnasium in Tübingen, Allgemeine Hochschulreife mit den Leistungskursen Mathematik und Physik

Zivildienst

1994 – 1995	Universitäts-Augenklinik Tübingen, Abteilung II, Sektion für visuelle Sensorik bei Prof. Dr. med M. FAHLE

Studium

1995 – 2002	Studium der Humanmedizin an der Universität Tübingen
	Tätigkeit in der Fachschaft Medizin; Studentischer Vertreter in Fakultätsrat und Studienkomission der Fakultät sowie im Senat der Universität
2001	Praktisches Jahr in Neurologie (Universität Tübingen & Brown University, Providence RI, USA), Innere Medizin (Brown University) und Chirurgie (Universidad Mayor de San Simón, Cochabamba, Bolivien)
14 / 11 / 2002	Ärztliche Prüfung
1997 – 1999	Zweitstudium der Physik mit Nebenfach Informatik
1999	Vordiplom in Physik
1999 – 2003	Master-Studiengang »Graduate School of Neural & Behavioural Sciences - International Max Planck Research School« an der Universität Tübingen

Dissertation

2004 – 2005	Neurologische Klinik, Abteilung für Kognitive Neurologie, Doktorvater: Prof. Dr. med H.-P. THIER
2008	Publikation: »How precise is gaze following in humans?«. *Bock SW, Dicke P, Thier P.* Vision Research 2008 Mar;48(7):946-57.

Beruf

2003 – 2004	Arzt im Praktikum, Neurologische Klinik, Tübingen
2004	Approbation als Arzt
seit 2004	Assistenzarzt / Wissenschaftlicher Mitarbeiter der Neurologischen Klinik am Universitätsklinikum Tübingen